Journal of Nuclear Medicine, published on July 12, 2018 as doi:10.2967/jnumed.118.214833

^{68}Ga-PSMA is a novel PET-CT tracer for imaging of hepatocellular carcinoma: A prospective pilot study

Short title: ^{68}Ga-PSMA PET-CT in HCC

Mikhail Kesler[1], Charles Levine[1], Dov Hershkovitz[2,3], Eyal Mishani[4], Yoram Menachem[5], Hedva Lerman[1,3], Yaniv Zohar[6], Oren Shibolet*[3,5], Einat Even-Sapir*[1,3].

[1]Department of Nuclear medicine, Tel Aviv Sourasky Medical Center, Tel Aviv, Israel.
[2]Department of Pathology, Tel Aviv Sourasky Medical Center, Tel Aviv, Israel.
[3]Sackler school of Medicine, Tel Aviv University, Tel Aviv, Israel.
[4]Cyclotron Unit, Hadassah Hebrew University Hospital, Jerusalem, Israel.
[5]Department of Gastroenterology, Tel Aviv Sourasky Medical Center, Tel Aviv, Israel.
[6]Department of pathology, Rambam Medical Center, Haifa, Israel.
*Equal contribution

Corresponding author:
Einat Even-Sapir M.D, PhD
Address: 62431, Weizmann St 6, Tel Aviv, Israel. Department of Nuclear medicine. Tel Aviv Sourasky Medical Center.
Telephone number: +972-52-426-6547, +972-3-697-3432.
Fax number: +972-3-697-3895.
E-mail address: evensap@tlvmc.gov.il

First author:
Mikhail Kesler M.D.
Address: 62431, Weizmann St 6, Tel Aviv, Israel. Department of Nuclear medicine. Tel Aviv Sourasky Medical Center.
Telephone number: +972-52-307-2635, +972-3-697-3432.
Fax number: +972-3-697-3895.
E-mail address: mikhailk@tlvmc.gov.il

The word count of the manuscript: 4005.

ABSTRACT

Background: ^{68}Ga-Prostate Specific Membrane Antigen (^{68}Ga-PSMA), a positron emission tomography (PET) tracer that was recently introduce for imaging of prostate cancer, may accumulate in other solid tumors including Hepatocellular Carcinoma (HCC). The aim of the study was to assess the potential role of ^{68}Ga-PSMA PET-Computed Tomography (CT) for imaging of HCC.

Material and methods: A prospective pilot study in seven patients with HCC with 41 liver lesions: 37 suspected malignant lesions (tumor lesions) and 4 regenerative nodules. For each liver lesion, uptake of ^{68}Ga-PSMA and ^{18}F-FDG uptake were measured [standard uptake value (SUV) and lesion-to-liver background ratios (TBR-SUV)], and correlated with dynamic characteristics (HU and TBR-HU) obtained on contrast enhanced CT data. Immunohistochemistry staining of PSMA in the tumor tissue was analyzed in samples obtained from 5 patients with HCC and compared to control samples from 3 patients with prostate cancer.

*Results***:** Thirty-six of the 37 tumor lesions and none of the regenerative nodules showed increased ^{68}Ga-PSMA uptake while only 10 lesions were ^{18}F-FDG avid. Based on contrast enhancement, tumor lesions were categorized into 27 homogeneously enhancing lesions, nine lesions with "mosaic" enhancement composed of enhancing and non-enhancing regions in the same lesion and a single non-enhancing lesion, the latter being the only non-^{68}Ga-PSMA avid lesion.

Using the Mann-Whitney test, ^{68}Ga-PSMA uptake was found significantly higher in enhancing tumor areas compared to non-enhancing areas and in contrast, ^{18}F-FDG uptake was higher in non-enhancing areas, $P<0.001$ for both. ^{68}Ga-PSMA uptake (TBR

SUVmax) was found to correlate with vascularity (TBR-HU) (Spearman r=0.866, p<0.001).

Immunohistochemistry showed intense intra-tumoral microvessel staining for PSMA in HCC, in contrast with cytoplasmic and membranous staining, mainly in the luminal border, in prostate cancer samples. In two of the study patients ^{68}Ga-PSMA PET-CT identified unexpected extrahepatic metastases. Four regenerative liver nodules showed no increased uptake of either of the PET tracers.

Conclusion: ^{68}Ga-PSMA PET-CT is superior to ^{18}F-FDG PET-CT in imaging patients with HCC. HCC lesions are more commonly hypervascular taking up ^{68}Ga-PSMA in tumoral micro-vessels. ^{68}Ga-PSMA PET-CT is a potential novel modality for imaging patients with HCC.

Key words: Hepatocellular carcinoma, PSMA, FDG, PET-CT

INTRODUCTION

Hepatocellular carcinoma (HCC) accounts for about 80% of all primary liver cancer. It is the fifth most common cancer worldwide, and the third cause of cancer related mortality (*1*). Cirrhosis due to viral hepatitis and non-alcoholic fatty liver disease are leading risk factors for HCC *(2*). The disease is confined initially to the liver; however, the incidence of remote metastases from HCC was reported to reach as high as 30% *(3*).

Current guidelines of the American association for the study of liver disease and the European association for the study of the liver recommend HCC surveillance with abdominal ultrasound every 6 months in patients at high risk of developing the disease. Patients diagnosed in early stages of the tumor are eligible for potentially curative therapy. Early diagnosis and accurate staging are therefore critical for favorable prognosis. Curative intent therapies for HCC include surgical resection, liver transplantation and in small tumors radio-frequency ablation *(4).*

Imaging of HCC at diagnosis is challenging and assessment of HCC recurrence following treatment is even harder, confounded by coagulative necrosis, hematomas, abscesses and fluid or bile collections *(5).*

Positron emission tomography (PET) using ^{18}F-Flurodeoxyglucose (^{18}F-FDG) has a limited role in evaluating patients with HCC as this tumor type is ^{18}F-FDG–avid in less than half of the cases *(6).* ^{68}Ga-Prostate-specific membrane antigen (^{68}Ga-PSMA) is a PET tracer recently introduced for the imaging of patients with high-risk prostate cancer at diagnosis and in patients with biochemical failure post treatment *(7).* Several case reports have described incidental increased uptake of ^{68}Ga-PSMA in other solid tumors

(8). We recently performed ^{68}Ga-PSMA PET-CT in a patient with prostate cancer noticing increased uptake of the tracer at the primary prostate cancer site, and additional ”hot” liver lesions (Figure. 1). The latter lesions were confirmed to be HCC by biopsy.

This case prompted us to conduct a prospective pilot study in order to explore the potential role of ^{68}Ga-PSMA PET-CT in HCC. ^{68}Ga-PSMA and ^{18}F-FDG PET-CT studies were performed in patients with HCC and compared with hemodynamic criteria derived from contrast enhanced (ce) CT and MR. We also assessed immunohistochemistry of PSMA expression in biopsy samples obtained from patients with HCC and patients with prostate cancer as control.

MATERIALS AND METHODS

Patient characteristics

PET-CT studies were performed in seven patients with HCC including five men and two women, 39-68 years of age. The study was approved by the institutional Review Board and patients signed a written informed consent. Six patients were newly diagnosed and one was after transarterial chemoembolization (TACE) of the right liver lobe. None of the patients had a known extrahepatic spread prior to PET-CT. Patients' characteristics are summarized in Table 1.

PET-CT Scan

All patients underwent two PET-CT scans; ^{68}Ga-PSMA-PET-ceCT and ^{18}F-FDG-PET-CT one to five days apart, using a Discovery 690 scanner (GE Healthcare). We

have used ^{68}Ga-PSMA with the precursor PSMA-11 (GMP), ABX (Radeberg, Germany). Administered doses were 148 Mbq 68Ga-PSMA and 444 Mbq ^{18}F-FDG. CT acquisition parameters were 100, 120 or 140 keV depending on patient habitus. PET reconstruction included time of flight; three iterations, 18 subsets with the filter cut-off set at 6.4; a standard z-axis filter; matrix size of 256 and Q Clear image reconstruction.

Correlation of PET findings and contrast enhancement on CT and MR

PET-CT data was interpreted by a single experienced expert (EES). Liver sites showing uptake higher than liver background activity were considered abnormal lesions. Standardized uptake values (SUV) of both the liver parenchyma (background) and hepatic lesions using a similar region of interest (ROI) were measured. Target-to-background ratios (TBR) were calculated.

All patients had ceCT available for correlation (the CT part of PET-CT as well as separately done CT). Three patients had also MR available for correlation, all reviewed by a radiologist, experienced in CT and MR body imaging (CL). On ceCT data, Hounsfield Units (HU) measured in the lesions and in the background parenchyma was recorded and TBR-HU was calculated. Liver lesions identified on ceCT and MR data were categorized as being suspicious of being malignant (tumor lesions), if they showed contrast enhancement and early portal washout, if they took up either tracer and if they grew compared to previous scans. Lesions were further defined as hypervascular or hypovascular. Hypervascular lesions were those showing prominent enhancement on the hepatic arterial dominant phase. Hypovascular lesions were those showing minimal enhancement on the hepatic arterial dominant phase and hypointensity compared to

liver background on delayed phases. Hypervascular lesions were subcategorized as being homogeneous or heterogeneous (“mosaic” pattern) where enhancing and non-enhancing regions were found in the same lesion. Based on contrast enhancement, tumor areas were sub categorized as enhancing and non-enhancing.

Extrahepatic lesions found on PET-CT were also recorded.

Immunohistochemistry of PSMA expression in HCC and in prostate cancer samples

A biopsy sample from liver tumor sites was available for assessment of PSMA expression in five patients with HCC; three patients from our cohort and two additional HCC patients that did not undergo PET-CT but had a CT study. For comparative purposes sampled from three patients with prostate cancer, were also analyzed. One 4mm slide was used for immunohistochemical staining. A slide of prostatic adenocarcinoma was used as internal control. Immunostaining was performed using the monoclonal anti–PSMA antibody (NCL–L–PSMA, Novocastra, New Castle, United Kingdom) at a 1:80 dilution on the Ventana BenchMark XT automated slide stainer (Ventana Medical Systems, Tucson, AZ, USA).

PSMA expression was evaluated by two experienced pathologists (D.H; Y.Z). Any reactivity in either tumor cells or neoplastic vessels was considered positive. In the case of heterogeneous staining, the predominant pattern was recorded.

Statistical analysis

SPSS software was used for all statistical analyses (IBM SPSS Statistics for windows, version 25, IBM corp., Armonk, NY, USA, 2017). Variables were evaluated for normal distribution using histogram and were recorded as median and interquartile range. These variables included the HU and TBR-HU in the lesion on ceCT and the minimum and maximum values of SUV and TBR-SUV for both ^{68}Ga-PSMA and ^{18}F-FDG on PET data. Uptake values of either of the tracers in enhancing and in non-enhancing lesions were compared using Mann-Whitney test. The correlation between CT contrast enhancement and PET tracers uptake was obtained by spearman correlation coefficient. After being tested to meet the expectations, linear regression was used to illustrate graphically the correlation between ^{68}Ga-PSMA uptake (TBR-SUV max) and vascularity (TBR-HU).

All statistical tests were two sided. A p value less than 0.05 was considered as statistically significant.

RESULTS

Imaging

Forty-one abnormal liver lesions were detected on CT and MR imaging including 37 lesions considered to be tumor lesions according to the pre-specified criteria and four regenerative nodules. One patient had a solitary lesion, and six had multifocal or infiltrative disease. Table 2 summarizes the ^{68}Ga-PSMA and ^{18}FDG-avidity of tumor lesions and whether enhancing on ceCT and/or MR.

Thirty-six of the 37 tumor lesions showed higher ^{68}Ga-PSMA uptake than the background liver uptake. Twenty-eight of the tumor lesions showing increased ^{68}Ga-PSMA uptake were non-^{18}FDG- avid (Figure 2) and eight showed avidity of both tracers. All lesions showing ^{68}Ga-PSMA avidity were associated with contrast enhancement on CT and/or MR representing hyper-vascularity, 27 with homogeneous enhancement and 9 with "mosaic" pattern composed of enhancing and non-enhancing areas (Figure 3). The single HCC lesions that did not show increased ^{68}Ga-PSMA uptake showed only mild peripheral contrast enhancement on CT but was primarily non-enhancing. It accumulated ^{18}FDG. Several HCC lesions illustrated co-existing avidity for PET tracers and contrast enhancement (Figure 4).

Table no 3 summarizes the uptake values of the two PET tracers and the vascularity presented on CT in all lesions as well as in the various areas within the lesion in case of mosaic lesions. Vascularity was expressed as mean HU and TBR-HU on CT, and tracer uptake by minimum and maximum SUV and TBR-SUV for both, ^{68}Ga-PSMA and ^{18}F-FDG.

Table no 4 summarizes the median and interquartile (IQR 25%-75%) of HU and uptake values of ^{68}Ga-PSMA and ^{18}F-FDG in enhancing and non-enhancing tumor areas. Using the Mann-Whitney test ^{68}Ga-PSMA uptake was found significantly higher in enhancing tumor areas compared to non-enhancing areas and in contrast, ^{18}F-FDG uptake was higher in non-enhancing areas, $P<0.001$ for both comparisons.

^{68}Ga-PSMA uptake (^{68}Ga-PSMA TBR-SUV max) was found to correlate with vascularity (TBR-HU) (Spearman $r=0.866$, $p<0.001$) and on linear regression analysis ($R^2=0.752$), (Figure 5).

The four liver lesions identified on CT as being hypodense and negative on PET with any of the tracers, were regenerative nodules remaining unchanged on follow-up imaging. The latter showed similar uptake to the surrounding liver parenchyma.

In order to assess potential differential ^{68}Ga-PSMA uptake in cirrhotic liver tissue, we compared ^{68}Ga-PSMA uptake in the non-tumor liver parenchyma in patients with (N=4) and without cirrhosis (n=3) and found no difference (^{68}Ga-PSMA SUVmean 3.3 (2.5-3.8) and 3.9 (3.2-4.4); respectively)

Two of the 7 patients (pt 1 and 7), had unexpected extrahepatic metastatic lesions on ^{68}Ga-PSMA PET-CT. Patient 1 had increased uptake in a right adrenal mass. Treatment with liver radio-embolization which was the initial treatment plan was altered to a systemic treatment with Sorafenib, a kinase inhibitor, and palliative radiotherapy to the adrenal. On follow up CT two months later the adrenal mass increased in size. The patients died 7 months later.

In patient 7 (Figure 6) a peritoneal implant and bone marrow involvement were identified on PSMA PET-CT. The implant was seen also on MRI. The patient died of advanced HCC 6 weeks later.

Immunohistochemistry

In three out of the five HCC samples analyzed intense intra-tumoral microvessel staining for PSMA was noted. No staining was identified in the epithelial tumor cells (Figure 7a). The tumor biopsy sites showing intense PSMA staining were enhanced on CT (HU of 114, 99 and 140 and TBR-HU of 2,1.6 and 1.6) with increased ^{68}Ga-PSMA uptake (Table 5), while the two negative areas were those obtained from non-enhancing

lesions (HU of 53 and 67 and TBR-HU of 0.6 and 0.8). The latter two samples were obtained in patients who had only CT. In contrast, in the prostate cancer control, staining for PSMA showed cytoplasmic and membranous positivity, mainly in the luminal boarder, however blood vessels were negative for PSMA staining (Figure 7b).

DISCUSSION

^{68}Ga-PSMA is a PET tracer recently introduced for PET-CT imaging of patients with prostate cancer. Its accumulation in prostate cancer tumor sites is the result of the overexpression of PSMA in the tumor cells *(7).*

Incidental uptake of ^{68}Ga-PSMA has been described in other solid tumors, including case reports of HCC (*9-11*). In the current prospective pilot study, we investigated the uptake of ^{68}Ga-PSMA and of the routinely used ^{18}F-FDG tracers in patients with HCC and compared it to contrast enhancement on CT and/or MR in a total of 41 liver lesions detected in 7 patients. We also assessed by immunohistochemistry the location of PSMA staining in the tumoral tissue.

Imaging of liver lesions in cirrhotic patients is complex and challenging. The cirrhotic liver acquires a nodular architecture with altered vascularity, making it hard to differentiate regenerative nodules from early HCC and metastases from other primary tumors. The challenge is even greater in patients that undergo ablative therapies to known HCC lesions. This complexity has resulted in the development of several staging algorithms including Response Evaluation Criteria In Solid Tumors (RECIST), modified RECIST and the Liver Reporting & Data System (LI-RADS score). These scores are frequently revised and are the focus of intense discussions *(12-15).*

Traditional imaging methods used in HCC patients are ultrasound (+/- contrast) and contrast enhanced multiphasic CT or MR. Each method has its shortcomings, with a major one being a lack of correlation between radiologic appearance and biological activity.

PET-CT has so far not played a major role in diagnosis or surveillance of HCC and ^{18}F-FDG, the most commonly used tracer, is not routinely used in the initial workup of HCC. ^{18}F-FDG PET is taken up by metabolically active cells and thus, tumor cells should theoretically show higher avidity to the isotope than normal cells. Despite this biologic reasoning, only a minority of HCCs take up ^{18}F-FDG *(16)*. Our group recently reviewed data on ^{18}F-FDG PET-CT in HCC. The data suggest that ^{18}F-FDG PET-CT is a stronger predictor of prognosis and is superior to assessment of tumor size or number of tumor nodules (as defined by the Milan criteria). This may have a direct impact on transplant outcome. ^{18}F-FDG PET–CT avidity in metabolically active tumors in patients planned for liver transplantation, resection or ablation may identify patients at risk for recurrence after each procedure *(6).* Furthermore, PET-CT may identify distant metastases that are hard to discover using conventional imaging.

Although data on the use of PET -CT imaging in HCC is promising it is not ready for prime time. It is based on small size, retrospective reports, with variable criteria of interpreting PET-CT findings. Perhaps the most prominent problem is that ^{18}F-FDG is not taken up by all tumors. Several studies showed suboptimal sensitivity (< 50%) of this modality for detection of new HCCs, being inferior to CT. This was attributed to the fact that tumor metabolic activity was similar to adjacent liver tissue.

Recognizing the importance of functional PET imaging, a search for new tracers has been on going. A preliminary report showed that dual tracer (^{11}C-acetate and ^{18}F-FDG) PET-CT was a highly sensitive tool for the detection of HCC, reaching approximately 94-95% sensitivity and 100% specificity, as compared with much lower sensitivity rates for contrast CT (detection rates of 67.6% and 37.5% for patients undergoing liver transplant and resection, respectively) *(17).*

The preliminary results of the current pilot study show encouraging results for ^{68}Ga-PSMA as a PET tracer for imaging of HCC. All but a single tumor lesion were associated with higher tracer uptake than that of the surrounding liver parenchyma with a mean uptake 3.6 times higher than that of the background liver. In contrast, only 10 of the malignant lesions were ^{18}F-FDG avid. Increased ^{68}Ga-PSMA uptake identified unexpected metastatic lesions in bone marrow, adrenal and an abdominal implant. Explanation for increased ^{68}Ga-PSMA uptake in HCC comes from the results of immunohistochemistry analysis showing PSMA staining of endothelial cell lining of tumor penetrating vessels. These findings are compatible with previous reports suggesting that nearly 95% of hepatocellular carcinomas stain positive for PSMA in the tumor vasculature *(18-20).*

Conway et al. recently showed that PSMA plays a major role in regulating angiogenesis. The process was markedly reduced in mice deficient in PSMA. Its function was mediated via a regulatory loop that modulates laminin-specific integrin signaling and GTPase-dependent, p21-activated kinase 1 (PAK-1) activity *(21).*

Zhu et al. suggested that the process of endothelial cell recruitment to HCC occurs early and throughout the process of hepatic tumorogenesis making an endothelial cell tracer an ideal marker of early disease *(22).*

HCC is a usually a highly vascular tumor characterized by early neo-angiogenesis, growth of functional collateral arteries covered with smooth muscle cells from pre-existing arteries. HCC is mainly supplied by branches of the hepatic artery, while in normal liver parenchyma, regenerative and dysplastic nodules are mainly supplied by the portal vein *(23).* Typically, in the arterial phase, there is minimal or no enhancement of the liver parenchyma and strong enhancement of hyper-vascular HCC lesions. During the delayed (portal) phase, there is rapid wash out of contrast from the tumor. These typical radiologic features are incorporated into the clinical practice guidelines *(4),* allowing for the diagnosis of HCC in cirrhotic patients without the need for biopsy. Enhancement on contrast-enhanced CT imaging was shown to correlate with microvessel density *(23).* Larger lesions are hypervascular unless rapid excessive tumor growth and further dedifferentiation occur. Then arterial flow may diminish with larger areas of necrosis *(24).*

The results of the current study suggest a close correlation between intra-tumoral microvessel staining for PSMA , increased ^{68}Ga-PSMA on PET and lesion vascularity expressed on contrast enhanced CT. Enhancing and non-enhancing lesions differed significantly in uptake of PET tracers. While enhancing lesions showed a higher ^{68}Ga-PSMA uptake compared to non-enhancing lesions, the latter showed a significantly higher uptake of ^{18}F-FDG. In Mosaic lesions composed of islands of contrast

enhancement, also ^{68}Ga-PSMA showed heterogeneity with increased uptake corresponding to the areas of high HU.

Our study has several limitations. The cohort is small with only seven patients included. However, 41 liver lesions were identified on CT/MR and were available for assessment.

Also, our study was an open study of patients with known HCC identified as HCC using "conventional" imaging prior to being enrolled. Thus the efficacy of ^{68}Ga-PSMA PET-CT in diagnosing tumors that does not follow the strict imaging criteria of HCC or its role in reducing the need for biopsies, is still questionable. Furthermore, the important distinction between early HCC and regenerative nodules needs to be validated.

It should also be remembered that in cirrhotic patients with a liver mass, current guidelines and clinical practice follows several imaging steps before biopsy is performed. PET imaging may be an early and cost saving tool in this scenario.

Our findings raise a potential role of ^{68}Ga-PSMA PET-CT in staging of patients with HCC encouraging assessing its role a larger patient's cohort.

DISCLOSURE

No potential conflict of interest relevant to this article was reported.

REFERENCES

1. Mittal S, El-Serag HB. Epidemiology of hepatocellular carcinoma: consider the population. *J Clin Gastroenterol.* 2013;47(suppl):s2-s6.

2. Zhu RX, Seto WK, Lai CL, et al. Epidemiology of hepatocellular carcinoma in the Asia-Pacific region. *Gut Liver.* 2016;10:332-339.

3. Lin CY, Chen JH, Liang JA, et al. 18F-FDG PET or PET/CT for detecting extrahepatic metastases or recurrent hepatocellular carcinoma: a systematic review and meta-analysis. *Eur J Radiol.* 2012;81:2417-2422.

4. European Association for the Study of the Liver. EASL clinical practice guidelines: management of hepatocellular carcinoma. *J Hepatol.* 2018;69:182-236.

5. Agnello F, Salvaggio G, Cabibbo G, et al. Imaging appearance of treated hepatocellular carcinoma. *World J Hepatol*. 2013;5:417-424.

6. Asman Y, Evenson AR, Even-Sapir E, et al. [18F]fludeoxyglucose positron emission tomography and computed tomography as a prognostic tool before liver transplantation, resection, and loco-ablative therapies for hepatocellular carcinoma. *Liver Transpl.* 2015;21:572-580.

7. Rauscher I, Maurer T, Fendler WP, et al. 68Ga-PSMA ligand PET/CT in patients with prostate cancer: How we review and report. *Cancer Imaging.* 2016;16:14.

8. Patel D, Loh H, Le K, et al. Incidental detection of hepatocellular carcinoma on 68Ga-labeled prostate-specific membrane antigen PET/CT. *Clin Nucl Med.* 2017;42:881-884.

9. Taneja S, Taneja R, Kashyap V, et al. 68Ga-PSMA uptake in hepatocellular carcinoma. *Clin Nucl Med.* 2017;42:e69-e70.

10. Soydal C, Alkan A, Ozkan E, et al. Ga-68 PSMA accumulation in hepatocellular carcinoma. *Gastroenterol Pancreatol Liver Disord.* 2016;4:1-1.

11. Sasikumar A, Joy A, Nanabala R, et al. (68)Ga-PSMA PET/CT imaging in primary hepatocellular carcinoma. Eur J Nucl Med Mol Imaging. 2016;43(4):795-796.

12. Ramalho M, Matos AP, AlObaidy M, et al. Magnetic resonance imaging of the cirrhotic liver: diagnosis of hepatocellular carcinoma and evaluation of response to treatment – Part 1. *Radiol Bras.* 2017;50:38-47.

13. Lyu N, Kong Y, Mu L, et al. Hepatic arterial infusion of oxaliplatin plus fluorouracil/leucovorin vs. sorafenib for advanced hepatocellular carcinoma. *J Hepatol.* February 20, 2018 [Epub ahead of print].

14. Choi MH, Park GE, Oh SN, et al. Reproducibility of mRECIST in measurement and response assessment for hepatocellular carcinoma treated by transarterial chemoembolization. *Acad Radiol.* March 16, 2018 [Epub ahead of print].

15. Kielar AZ, Chernyak V, Bashir MR, et al. LI-RADS 2017: an update. *J Magn Reson Imaging.* April 6, 2018 [Epub ahead of print].

16. Li YC, Yang CS, Zhou WL, et al. Low glucose metabolism in hepatocellular carcinoma with GPC3 expression. *World J Gastroenterol.* 2018;24:494–503.

17. Larsson P, Arvidsson D, Björnstedt M, at al. Adding 11C-acetate to 18F-FDG at PET examination has an incremental value in the diagnosis of hepatocellular carcinoma. *Mol Imaging Radionucl Ther.* 2012;21:6–12.

18. Liu H, Moy P, Kim S, et al. Monoclonal antibodies to the extracellular domain of prostate-specific membrane antigen also react with tumor vascular endothelium. *Cancer Res.* 1997;57:3629-3634.

19. Chen Y, Dhara S, Banerjee SR, et al. A low molecular weight PSMA-based fluorescent imaging agent for cancer. *Biochem Biophys Res Commun.* 2009;390:624-629.

20. Mhawech-Fauceglia P, Zhang S, Terracciano L, et al. Prostate-specific membrane antigen (PSMA) protein expression in normal and neoplastic tissues and its sensitivity and specificity in prostate adenocarcinoma: an immunohistochemical study using mutiple tumour tissue microarray technique. *Histopathology*. 2007;50:472-483.

21. Conway RE, Petrovic N, Li Z, et al. Prostate-specific membrane antigen regulates angiogenesis by modulating integrin signal transduction. *Mol Cell Biol.* 2006;26:5310-5324.

22. Zhu H, Shao Q, Sun X, et al. The mobilization, recruitment and contribution of bone marrow-derived endothelial progenitor cells to the tumor neovascularization occur at an early stage and throughout the entire process of hepatocellular carcinoma growth. *Oncol Rep.* 2012;28:1217-1224.

23. Muto J, Shirabe K, Sugimachi K, et al. Review of angiogenesis in hepatocellular carcinoma. *Hepatol Res.* 2015;45:1-9.

24. Choi JY, Lee JM, Sirlin CB. CT and MR imaging diagnosis and staging of hepatocellular carcinoma: part I. Development, growth, and spread: key pathologic and imaging aspects. *Radiology.* 2014;272:635-654.

FIGURES

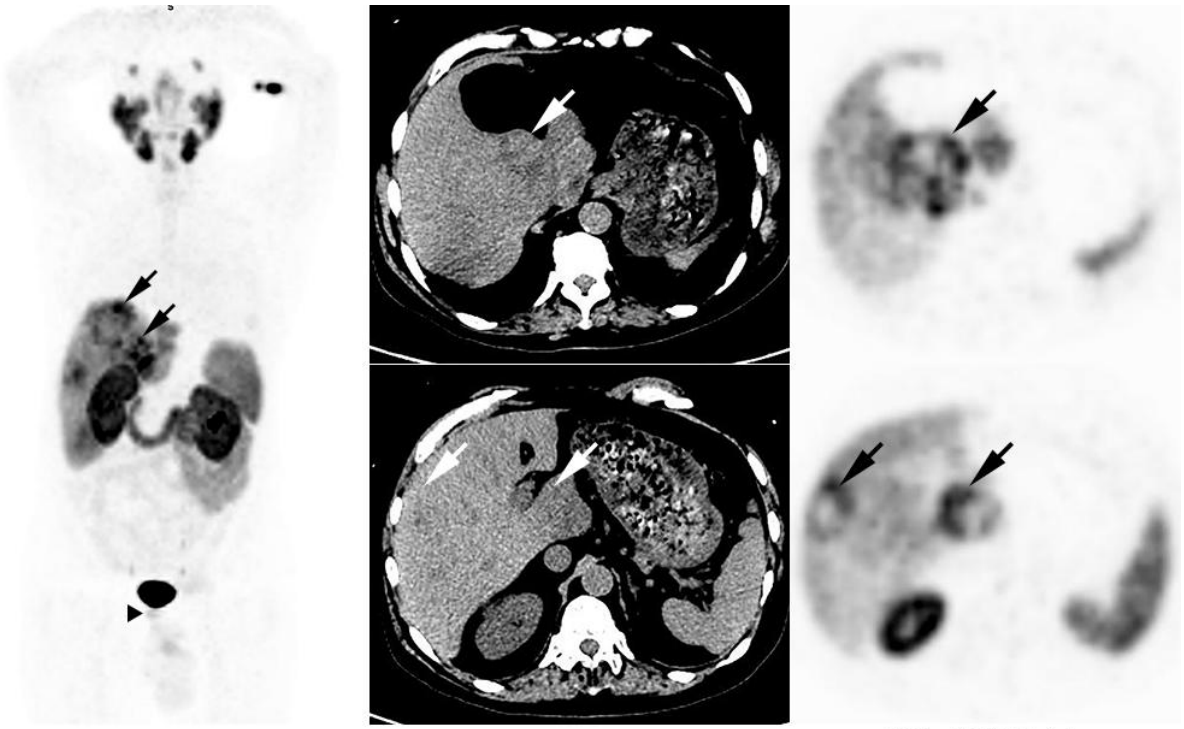

FIGURE 1. Incidental ^{68}Ga-PSMA–avid liver lesions detected in a patient referred for ^{68}Ga-PSMA PET-CT due to newly diagnosed high-risk prostate cancer. Uptake of ^{68}Ga-PSMA in prostatic cancer (arrow head) and liver lesions (arrow). Following the PET-CT findings unknown HCC was diagnosed.

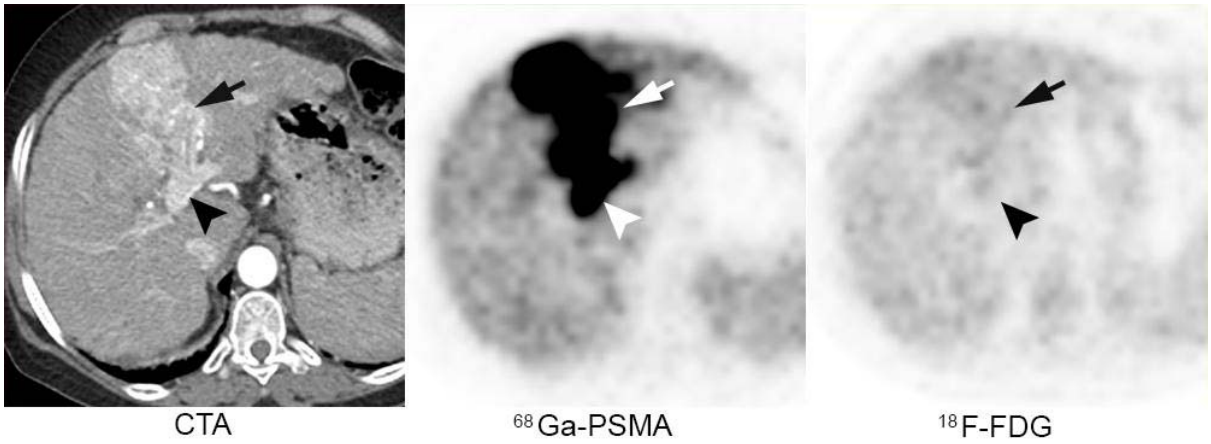

FIGURE 2. Enhancing HCC Increased uptake of ^{68}Ga-PSMA is seen in the tumor at the left liver lobe (arrow) as well as in a tumor thrombus in the left portal vein (arrow head). These lesions show no ^{18}F-FDG avidity.

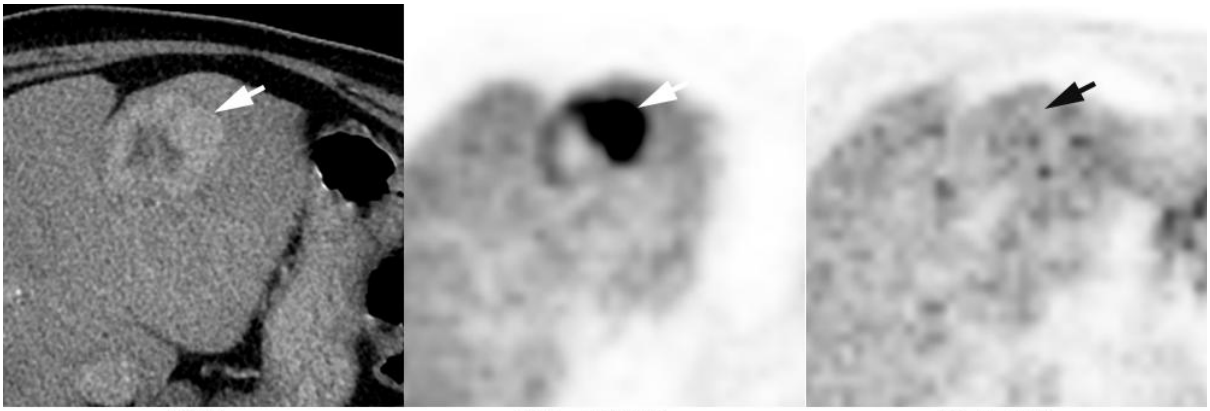

FIGURE 3. HCC lesion with "mosaic" contrast enhancement. Increased ^{68}Ga-PSMA uptake is identified only in the enhancing area (arrow). This HCC is non-^{18}F-FDG avid.

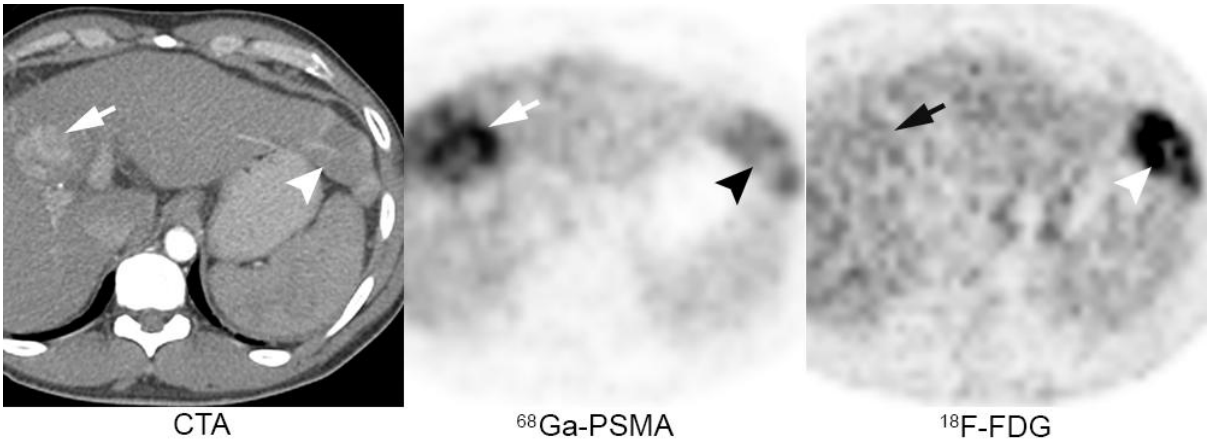

FIGURE 4. Co-existing ^{68}Ga-PSMA (arrow) and ^{18}F-FDG HCC (arrow head) lesions. Increased ^{68}Ga-PSMA uptake is seen in en enhancing tumor lesion.

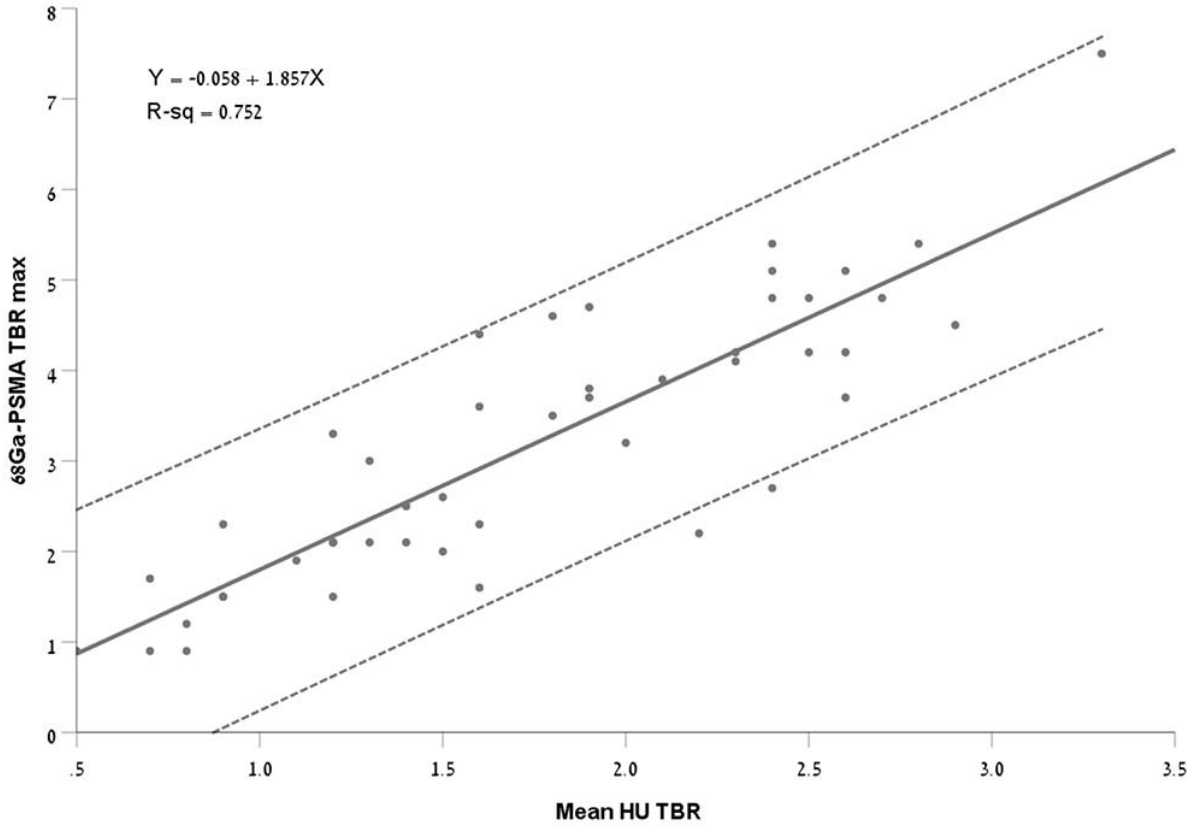

Figure 5. Linear regression and 95%CI correlating ^{68}Ga-PSMA uptake and vascularity in HCC.

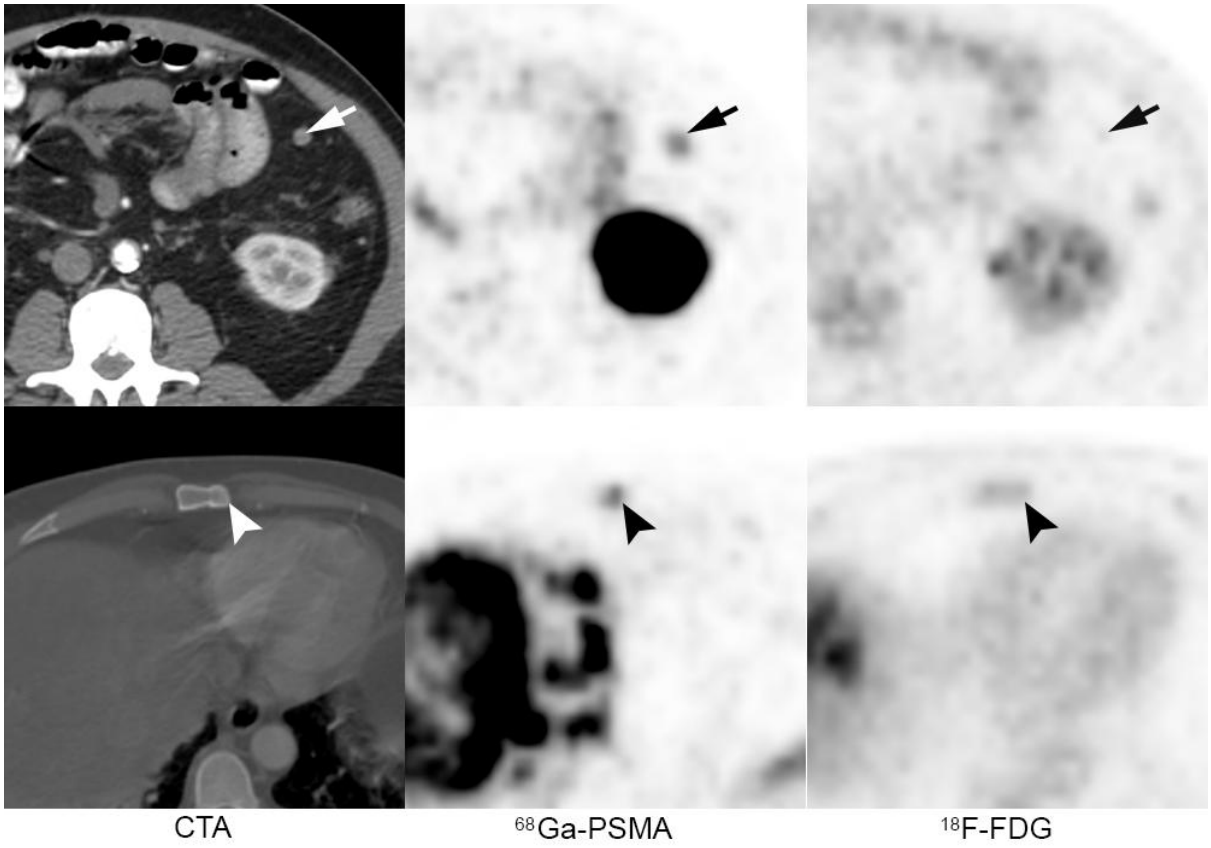

FIGURE 6. Unexpected bone metastasis in sternum (arrow head) and implant in the left upper quadrant (arrow) showing ^{68}Ga-PSMA uptake and not ^{18}F-FDG uptake.

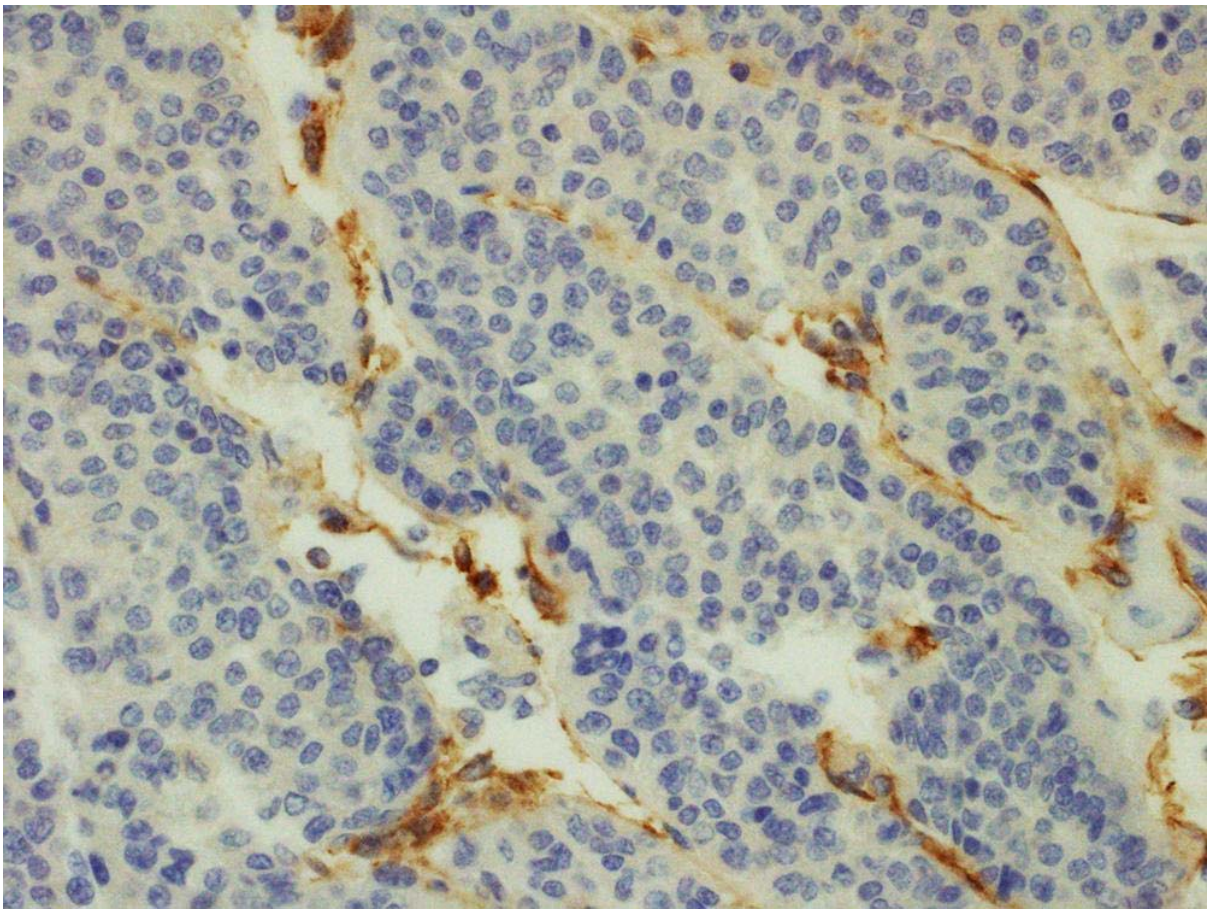

FIGURE 7a. Immunohistochemical analysis of hypervascular HCC. Intense intra-tumoral microvessel staining for PSMA (zoom x40).

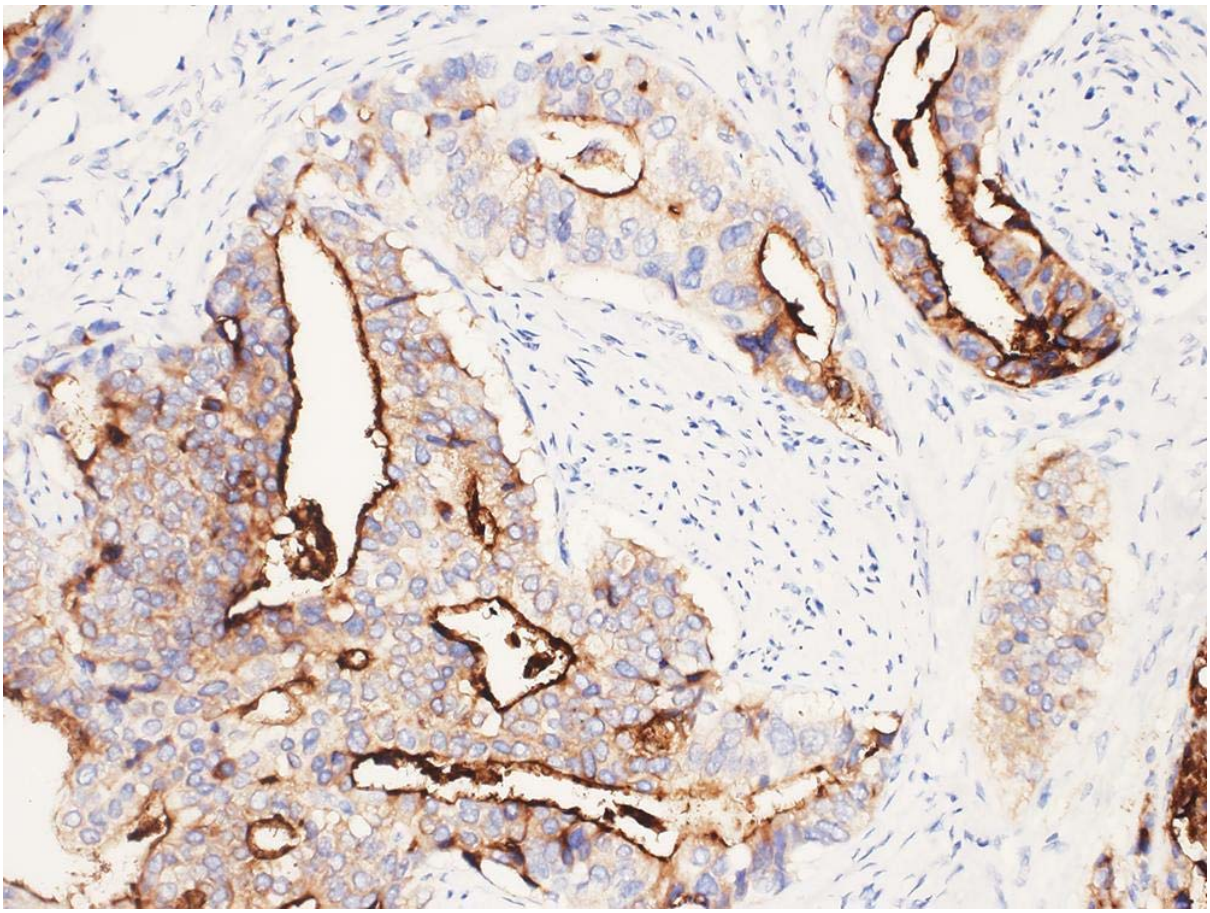

FIGURE 7b. Immunohistochemical analysis of the prostate cancer. Staining for PSMA showed cytoplasmic and membranous positivity, mainly in the luminal boarder, however blood vessels were negative for the staining (zoom x20).

TABLES

TABLE 1. Patients' characteristics.

Pt	Age (yr)	Sex	Stage of disease	Predisposing risk for HCC*	Chronic liver disease	Ch-P**	PS***	HTS****	AFP***** (ng/mL)
1	51	male	After TACE	HCV	Cirrhosis	B	1	T3	8
2	56	female	Initial staging	HBV	Cirrhosis	B	2	T3	46.6
3	62	female	Initial staging	HCV	Normal liver	A	0	T2	3648
4	59	male	Initial staging	HBV	Cirrhosis	B	1	T3	5336
5	38	male	Initial staging	HCV	Cirrhosis	B	1	T3	1800
6	69	male	Initial staging	HCV	Fatty Liver	A	1	T2	11
7	54	male	Initial staging	Familial HCC	Fatty Liver	A	1	T3	4000

* Predisposing disease for HCC: HCV: hepatitis C virus; HBV: hepatitis B virus.

** Ch-P: Child-Pugh score.

*** PS: Eastern Cooperative Oncology Group performance status.

**** HTS: Hepatic tumor stage based on morphologic imaging. Liver tumor stage: T2: solitary tumor with vascular invasion or multiple tumors (< 5 cm); T3: multiple tumors of any size involving a major branch of the portal vein or hepatic vein.

***** AFP: Alpha-fetoprotein.

TABLE 2. PET tracer's uptake and contrast enhancement on CT/MR of HCC liver lesions.

Pt	PSMA+ FDG -	Enhanced		PSMA+ FDG +	Enhanced		PSMA - FDG +	Enhanced	
		Hom*	Mos**		Hom	Mos		Hom	Mos
1	6	6	0	-	-	-	-	-	-
2	2	2	0	-	-	-	-	-	-
3	1	1	0	-	-	-	-	-	-
4	3	3	0	3	0	3	-	-	-
5	2	2	0	1	0	1	-	-	-
6	1	1	0	-	-	-	1	0	0
7	13	12	1	4	0	4	-	-	-

* Hom - homogenous.

** Mos - mosaic.

TABLE 3. Contrast enhancement, ^{68}Ga-PSMA and ^{18}F-FDG uptake in homogeneous HCC lesions and in areas within mosaic HCC lesions.

Pt	CT					^{68}Ga-PSMA				^{18}F-FDG			
	Lesion	Area within the lesion	E/N*	HU**		SUV		TBR-SUV		SUV		TBR-SUV	
				Mean	TBR***	min	max	min	max	min	max	min	max
1	1	1	E	114	2	9	11,7	3,1	3,2	1,4	1,8	1	0,9
	2	1	E	124,5	2,1	9,5	14,6	3,3	3,9	1,6	2,5	1,1	1,3
	3	1	E	128	2,2	5	8,2	1,7	2,2	1,6	2,1	1,1	1
	4	1	E	94,5	1,6	4,2	5,4	1,5	1,6	1,4	2,4	1	1,2
	5	1	E	89,7	1,5	7,8	9,5	2,7	2,6	1,6	2	1,1	1
	6	1	E	86,7	1,5	4,6	7,4	1,6	2	1,6	2,3	1,1	1,2
2	1	1	E	188,5	3,3	21	30,7	6,4	7,5	2,7	4,1	1,6	1,6
	2	1	E	144,5	2,4	6	11,1	1,8	2,7	2	3,1	1,2	1,2
3	1	1	E	99	1,6	10,5	17,5	3,3	3,6	3,8	6,5	2,5	3
4	1	1	E	117	1,3	9,1	13	3,4	3	1,8	2,8	1,1	1,2
	2	1	E	112	1,2	7,6	9,2	2,8	2,1	2,4	3,5	1,5	1,5
		2	N	84	0,9	2,9	6,4	1,1	1,5	6,4	9,4	4	3,9
	3	1	E	110,8	1,2	3,7	6,7	1,4	1,5	1,2	2,5	0,8	1
	4	1	E	77	0,9	4	6,6	1,5	1,5	2,8	3,2	1,8	1,3
		2	N	62	0,7	3,5	4,2	1,3	0,9	3,4	4,5	2,1	1,9
	5	1	E	110	1,2	9,2	14,7	3,4	3,3	1,9	2,5	1,2	1
		2	E	127,9	1,4	7,2	10,9	2,7	2,5	2	3	1,3	1,3
		3	N	71	0,8	2,6	3,9	1	0,9	2,7	2,9	1,7	1,2
	6	1	E	127	1,4	5,7	9,1	2,1	2,1	1,9	2,7	0,6	1,1
5	1	1	E	96,4	1,6	4,7	6,1	2,6	2,3	1,6	4,5	1,2	1,6
	2	1	E	109,8	1,8	7	9,6	3,9	3,5	1,7	2,7	1,3	0,9
	3	1	N	43,5	0,7	3,2	4,7	1,8	1,7	5,2	5,7	4	2
6	1	1	E	140	1,6	25,6	41,2	3,4	4,4	1,8	2,7	1	0,9
	2	1	N	62	0,5	3,7	8,3	0,5	0,9	5	7,3	2,9	2,4
7	1	1	E	75	1,9	11,4	11,9	4,2	3,7	2,4	3,8	1,3	1,4

	2	N	32,2	0,8	3,6	3,7	1,3	1,2	8,3	9	4,6	3,3
2	1	E	69,8	1,8	9,4	14,8	3,5	4,6	2,6	2,9	1,4	1,1
3	1	E	89,6	2,3	11,3	13	4,2	4,1	2,5	3,2	1,4	1,2
4	1	E	94	2,4	13,6	17,3	5	5,4	2,4	2,7	1,3	1
5	1	E	73	1,9	12,7	15	4,7	4,7	2,6	3	1,4	1,1
6	1	E	92	2,4	12,5	16,3	4,6	5,1	2,5	3,3	1,4	1,2
	2	N	36	0,9	3,2	7,2	1,2	2,3	3,1	3,9	1,7	1,4
7	1	E	76	1,9	10,2	12	3,8	3,8	2	3,7	1,1	1,4
8	1	E	91	2,3	9,5	13,5	3,5	4,2	1,8	2,7	1	1
9	1	E	115	2,9	10	14,3	3,7	4,5	2,3	3,2	1,3	1,2
	2	N	46	1,2	4,3	6,8	1,6	2,1	4	7,1	2,2	2,6
10	1	E	97	2,5	12	13,3	4,4	4,2	2,1	2,8	1,2	1
	2	N	43	1,1	4,6	6	1,7	1,9	4,2	6,1	2,3	2,3
11	1	E	96	2,5	8,2	15,3	3	4,8	2	3,9	1,1	1,7
12	1	E	104	2,7	9,9	15,5	3,7	4,8	2,4	3,2	1,3	1,2
13	1	E	101	2,6	9,8	16,3	3,6	5,1	2	2,9	1,1	1,1
14	1	E	93	2,4	10,4	15,4	3,9	4,8	1,8	2,5	1	1
15	1	E	110	2,8	9,5	17,3	3,5	5,4	2,5	3	1,4	1,1
16	1	E	100	2,6	8,5	11,7	3,1	3,7	2,5	3,7	1,4	1,4
	2	N	51	1,3	3,8	6,7	1,4	2,1	3	4,3	1,7	1,6
17	1	E	101	2,6	12	13,5	4,4	4,2	2	3,7	1,1	1,4

* E - Enhancing tumor areas; N - Non-enhancing tumor areas.
** HU - Hounsfield unit mean.
*** TBR - Tumor-to-background ratio.

TABLE 4. HU on ceCT and ^{68}Ga-PSMA and ^{18}F-FDG uptake on PET data in enhancing and in non-enhancing HCC areas. Variables are expressed as median and interquartile (IQR 25%-75%).

Enhancement on ceCT	No of areas	Mean HU	TBR-HU	68Ga-PSMA SUVmax	18F-FDG SUVmax	68Ga-PSMA TBR-SUVmax	18F-FDG TBR-SUVmax
Enhancing tumor areas	36	100.5 (91.3-114.8)	1.95 (1.5-2.5)	13.2 (9.5-15.4)	2.9 (2.6-3.5)	3.8 (2.5-4.7)	2.1 (1.6-2.8)
Non-enhancing tumor areas	10	48.5 (41.3-64.3)	0.85 (0.7-1.1)	6.2 (4.1-6.9)	5.9 (4.2-7.7)	1.6 (0.9-2.1)	1.2 (1-1.4)

TABLE 5. CT and PET characteristics of HCC biopsy sites showing intense intra-tumoral microvessel staining for PSMA on immunohistochemical analysis.

Pt	Pathology	HU	TBR-HU	68Ga-PSMA SUVmin	68Ga-PSMA SUVmax	18F-FDG SUVmin	18F-FDG SUVmax
1	Well differentiated HCC (G1)	114	2	9	11.7	1.4	1.8
3	Moderately differentiated HCC (G2)	99	1,6	10.5	17.5	3.8	6.5
6	Moderately differentiated HCC (G2)	140	1,6	25.6	41.2	1.8	2.7